JACS
JOURNAL OF THE AMERICAN CHEMICAL SOCIETY
Communication
pubs.acs.org/JACS

Stabilization of Graphene Sheets by a Structured Benzene/Hexafluorobenzene Mixed Solvent

Andrew J. Oyer,[†] Jan-Michael Y. Carrillo,[†,‡] Chetan C. Hire,[†] Hannes C. Schniepp,[∥] Alexandru D. Asandei,[†,¶] Andrey V. Dobrynin,[†,‡] and Douglas H. Adamson*[,†,¶]

[†]Institute of Materials Science, Polymer Program, University of Connecticut, Storrs, Connecticut 06269, United States
[‡]Physics Department and [¶]Chemistry Department, University of Connecticut, Storrs, Connecticut 06269, United States
[∥]Department of Applied Science, The College of William and Mary, Williamsburg, Virginia 23185, United States

Supporting Information

ABSTRACT: Applications requiring pristine graphene derived from graphite demand a solution stabilization method that utilizes an easily removable media. Using a combination of molecular dynamics simulations and experimental techniques, we investigate the solubliza-tion/suspension of pristine graphene sheets by an equimolar mixture of benzene and hexafluorobenzene (C_6H_6/C_6F_6) that is known to form an ordered structure solidifying at 23.7 °C. Our simulations show that the graphene surface templates the self-assembly of the mixture into periodic layers extending up to 30 Å from both sides of the graphene sheet. The solvent structuring is driven by quadrupolar interactions and consists of stacks of alternating C_6H_6/C_6F_6 molecules rising from the surface of the graphene. These stacks result in density oscillations with a period of about 3.4 Å. The high affinity of the 1:1 C_6H_6/C_6F_6 mixture with graphene is consistent with observed hysteresis in Wilhelmy plate measurements using highly ordered pyrolytic graphite (HOPG). AFM, SEM, and TEM techniques verify the state of the suspended material after sonication. As an example of the utility of this mixture, graphene suspensions are freeze-dried at room temperature to produce a sponge-like morphology that reflects the structure of the graphene sheets in solution.

The promise of graphene for material applications comes from its impressive electrical, thermal, and mechanical properties.[1−4] Thermal conductivities as high as ∼5,000 W/mK,[5] Young's modulus values of up to ∼1.0 TPa,[6] and breaking strengths of ∼40 N/m have been reported.[6] Practical applications utilizing these impressive properties, however, are limited.[1] One reason for this is the challenge of producing stable suspensions of graphene without introducing hard to remove stabilizers such as surfactants, polymers, high-boiling solvents, salts, or super acids.[1,7−10] Currently, the most commonly used approach involves the oxidation of graphite to graphite oxide (GO), followed by stabilization in water driven by sonication. This is often followed by chemical reduction, but the resultant graphene sheets contain high levels of defects.[2,11] For many applications, however, pristine sheets are required. Toward this end, advances have been made in the production of low defect density graphene sheets by controlled vapor deposition (CVD), an energy intensive process that is likely too costly for many applications.[7] Obtaining graphene from natural sources would appear to be a less expensive alternative.

In this communication we present a method for obtaining high-concentration suspensions of graphene material from both natural flake graphite and highly ordered pyrolytic graphite (HOPG). The solvents we use are low-molecular weight with low boiling temperatures, easily removable by simple evaporation. This solvent system, an equimolar of solution of benzene (C_6H_6) and hexafluorobenzene (C_6F_6), solidifies at 23.7 °C, with its solid structure consisting of alternating C_6H_6/C_6F_6 columns.[12] The boiling point of the mixture is approximately 78 °C, nearly the same as that of the pure solvents,[13] and is easily removed at moderate temperatures.[14] While independently both benzene and hexafluorobenzene have been shown to be less than optimal solvents for graphene solution stabilization,[15] their equimolar mixture provides a structured solvent fundamentally different than either solvent separately.

Equimolar solutions of C_6H_6/C_6F_6 were first studied and characterized in the 1960s,[14] and their structure has been explained by quadrupolar interactions.[16−18] Simulations of the charge densities of C_6H_6 and C_6F_6 indicate that they are complementary, with C_6F_6 having a localized, independent charge density on each F atom.[19] These charge densities give rise to interactions that have been successfully exploited in supramolecular[20,21] and polymer[22−24] chemistry and in the stabilization of liquid crystalline phases.[25] In this communication, we show that the ordering resulting from these interactions can be nucleated by graphene, inducing ordering above the bulk melting temperature, and we utilize this process for graphene stabilization.

Molecular dynamics simulations are used to highlight the unique properties of this mixed solvent. We perform molecular dynamics simulations of a graphene sheet immersed in water, C_6H_6, xylenes, heptane, C_6F_6, and various C_6H_6/C_6F_6 mixtures. The simulations are done using the NPT ensemble at T = 300 K and P = 1 atm, with details given in the Supporting Information (SI). Figure 1 shows the solvent density

Received: November 30, 2011
Published: March 13, 2012

   dx.doi.org/10.1021/ja211225p | J. Am. Chem. Soc. 2012, 134, 5018−5021

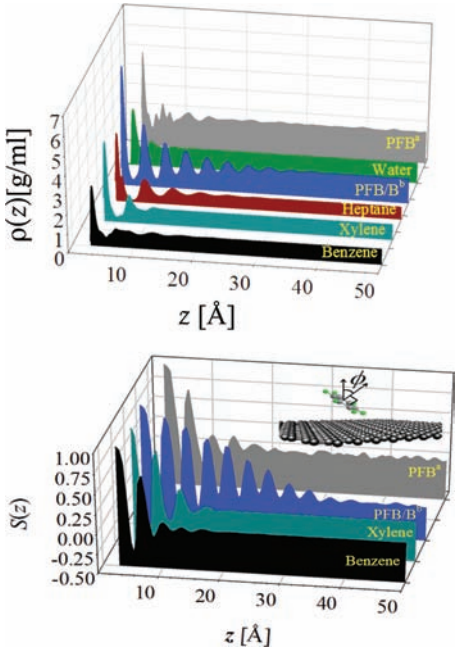

Figure 1. (Top) Solvent density distributions obtained from molecular dynamics simulations of a graphene sheet immersed into different solvents. (Bottom) Solvent orientational order parameter distribution in aromatic solvents. [a]Hexafluorobenzene. [b]Equimolar mixture of hexafluorobenzene and benzene.

distribution along the *z*-axis with the graphene sheet located in the *xy*-plane. Here we only show the density distribution along positive *z*-direction, but the density profile is symmetric and spans both sides of the graphene sheet. It is apparent that the graphene sheet induces a layered structure in the C_6H_6/C_6F_6 mixture, which is observed as density oscillations with a period of about 3.4 Å. This corresponds to the van der Waals diameter of the carbon atom. Some degree of ordering is also observed in C_6F_6 and heptane systems, but it is not as well pronounced as in the 1:1 C_6H_6/C_6F_6 mixture, where one can clearly identify at least eight peaks spanning up to 30 Å from the graphene surface. This long-range ordering is due to quadrupolar interactions between C_6H_6 and C_6F_6 molecules within stacks of alternating molecules.

Within the layers, molecules are oriented parallel to the graphene sheet. This can be seen in the lower panel of Figure 1, where the distribution of the orientational order parameter

$$S(z) = \frac{(3\langle\cos^2(\varphi(z))\rangle - 1)}{2} \quad (1)$$

is shown, with $\varphi(z)$ being the angle between the *z*-axis and normal to the plane of the carbon ring of the aromatic solvent molecule. Averaging over all orientations of solvent molecules with the center of mass located at distance *z* from a graphene surface is performed during the last stages of the simulation runs. Close to the graphene surface the value of the order parameter *S* approaches one. This value of the order parameter corresponds to a parallel alignment of the solvent molecules and graphene sheet. This is also clearly seen in the snapshot of the first-layer structure, shown in Figure 2.

The negative values of the order parameter *S* correspond to perpendicular orientations of the solvent molecules and graphene sheet (Figure 2). As in the case of the density distribution (Figure 1), the 1:1 C_6H_6/C_6F_6 mixture shows the

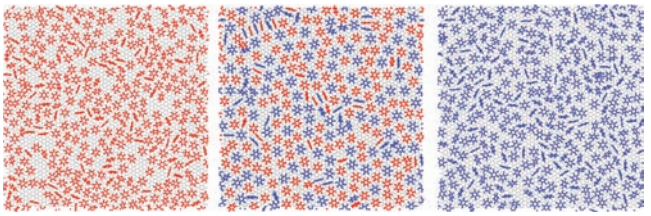

Figure 2. Snapshot of the first-layer structure relative to the graphene sheet for benzene (left), C_6F_6 (right), and the 1:1 molar mixture (center), with C_6F_6 molecule in blue and C_6H_6 in red.

longest orientational correlations between solvent molecules and the graphene sheet. While a high degree of orientational and translational order in the *z*-direction in the C_6H_6/C_6F_6 mixture is present, the snapshots of the first-layer structure (see Figure 2) do not show a high degree of lateral order. This is what one would expect for liquid crystalline ordering in mixtures of disklike molecules.

We also perform simulations during which a potential of the mean force between a large graphene sheet and a small graphene flake is calculated (details in SI).[26] In these simulations, a graphene flake is modeled by a G8 coronene-like molecule ($C_{384}H_{48}$). The simulations are performed at constant system temperature and volume, thus providing information about the change in the Helmholtz free energy of the system as a function of separation between the graphene sheet and graphene flake.

Simulations have shown qualitatively different graphene solubility in the 1:1 C_6H_6/C_6F_6 mixture and pure hexafluorobenzene as compared with that in benzene. In a 1:1 C_6H_6/C_6F_6 mixture and in pure hexafluorobenzene, the solvated graphene state has a lower Helmholtz free energy than does the layered graphene state. Thus, having both sides of a graphene sheet covered with solvent is more thermodynamically favorable than having two sheets in contact with each other. This is manifested in a positive change in the Helmholtz free energy upon graphene aggregation (or restacking), with ΔF = 838 kcal/mol for the 1:1 C_6H_6/C_6F_6 mixture and ΔF = 672 kcal/mol for hexafluorobenzene. The opposite trend is observed in benzene, with ΔF = −89 kcal/mol. Benzene is thus a poor solvent for graphene. The larger positive value of ΔF obtained for the 1:1 C_6H_6/C_6F_6 mixture confirms that the mixture is a better solvent for graphene than is the pure hexafluorobenzene or pure benzene, and that the mixed solvent is not simply a weighted average of the two. It is important to point out that one can still see a suspension of graphene in benzene after sonication. This is due to an energy barrier separating solvated and layered graphene states (see SI for details). Such suspensions are kinetically stable, and it will take some time for graphene sheets to aggregate and settle.

To confirm unique properties of 1:1 C_6H_6/C_6F_6 mixture experimentally, we employ a Wilhelmy plate method in order to observe the interaction of the solvent mixture with graphene surfaces. In this method, an HOPG sample is suspended from the beam of a balance, and a solvent is raised to the HOPG at a set rate (see SI for details). In the case of solvents that wet the HOPG surface, a wicking event occurs and is observed as an increase in the weight of the HOPG just before it enters the solvent and buoyant forces begin decreasing the observed weight (advancing). As the solvent is then removed from the HOPG (receding), the observed weight increases as the buoyant forces decrease, until the distance between the solvent

dx.doi.org/10.1021/ja211225p | *J. Am. Chem. Soc.* 2012, 134, 5018−5021

and the HOPG is zero and only the wicked solvent remains. As the HOPG moves above the solvent, the wicking ceases, and the weight decreases. The results of these weight vs distance[27,28] measurements show hysteresis, with the advancing weight being lower than the receding weight. The hysteresis is presented as the difference in the weights divided by the advancing weight, and is presented in Table 1.

Table 1. Hysteresis of Solvents with Graphene

solvent	average advancing weight gain (mg)	average receding weight retained (mg)	hysteresis[c]
C_6H_6	67.5	77.5	0.149
xylenes	46.5	53.0	0.140
heptane	51.0	57.0	0.118
C_6F_6[a]	60.0	64.5	0.075
NMP	92.5	107.5	0.162
C_6H_6/C_6F_6[b]	54.5	71.0	0.303

[a]Hexafluorobenzene. [b]Equimolar mixture of hexafluorobenzene and benzene. [c]Calculated as the difference of advancing and receding weight divided by advancing weight.

The source of hysteresis in such measurements has been thought in the past to arise from several possible sources: surface roughness, chemical nature of the surface, adhesion, rearrangement of the surface when in contact with the liquid, and chemical heterogeneity of the surface that causes pinning of the advancing or receding contact line.[27,29−34] As all of our measurements use the same HOPG sample, the condition of the surface cannot explain the hysteresis differences. Additionally, the structure of the HOPG surface is chemically homogeneous and will not rearrange, as is sometimes observed with polymeric surfaces. Therefore, the differences in hysteresis are attributed to differences in the adhesion of the various solvents to the graphene surface. While the average hysteresis for heptane, NMP, benzene, and xylenes is 0.142 ± 17%, for C_6F_6 it is 0.075 (47% lower than average), and for the C_6H_6/C_6F_6 mixture it is 0.303 (113% higher than average).

These differences are explained as resulting from the quadrupolar ordering observed in our simulations. Since both C_6F_6 and C_6H_6 associate with graphene via van der Waals interactions, the smaller van der Waals size of H as compared to F results in a larger adsorption energy for hydrogenated solvents as compared to C_6F_6. This is manifested in the smaller hysteresis of C_6F_6 in comparison with C_6H_6 or the other solvents. The monolayer closest to the graphene surface in the mixture, however, (see Figure 2), consists of both C_6H_6 and C_6F_6 molecules, allowing the next layer to associate with complementary quadrupoles. This continues for some distance, resulting in an increased mass of the solvent adhering to the graphene surface. The other solvents do not associate through quadrupolar interactions but rather through dispersion forces that are weaker than the complementary quadrupolar C_6H_6/C_6F_6 interactions. Therefore their hysteresis values lie between the larger retained mass of the mixture and the smaller retained mass of the poorly interacting C_6F_6.

Stable suspensions derived from the sonication of both natural flake graphite and HOPG are found to be stable for long periods of time with typical 50 mg/mL concentrations of natural flake graphite showing no signs of settling after sitting for more than one month. Figure 3 shows suspensions of natural flake graphite before and after sonication. After sitting for over a week, no settling is observed. Similar images of the

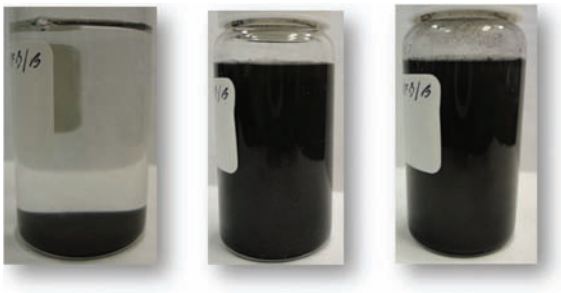

Figure 3. Natural flake graphite (50 mg/mL) in an equimolar solution of C_6H_6/C_6F_6. The picture on the left is of the mixture before sonication, the image in the middle is after sonication, and the picture on the right is the suspension after standing for more than one week.

component solvents are included in the SI, as is TEM and Raman data. Imaging these dark solutions suggest that they contain large flakes of pristine graphene rather than simply small fragments produced by sonication. Figure 4 shows AFM images of exfoliated sheets from both natural flake graphite and HOPG.

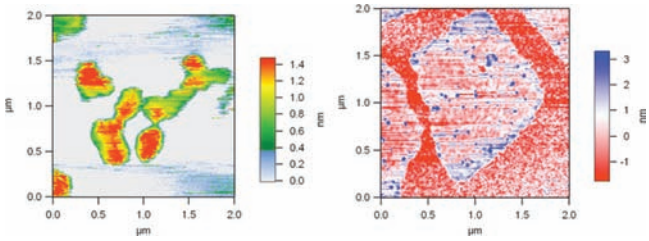

Figure 4. AFM images of graphene sheets prepared in the C_6H_6/C_6F_6 solvent mixture. The sheets are in the micrometer range for both natural flake graphite (left) as well as HOPG (right).

While exfoliating and suspending graphene sheets is a critical step toward many applications, the final material will likely need to be stabilizer free. One way to remove volatile stabilizing solvents while retaining the dispersed morphology is through freeze-drying, which has been shown to produce graphitic materials with high surface areas in systems that involve GO suspended in water,[35] or reduced GO in water with polymeric stabilizers.[36] Proposed applications for these materials include catalysis, drug release, biotechnology, and electronics.[37] In all previous work, water is used as the solvent, and due to the insolubility of graphene in water, it has been necessary to oxidize the graphene first, thus introducing defects that adversely affect the properties of the sheets. High-boiling solvents such as NMP and DMF are not suitable for freeze-drying due to their low vapor pressures. By contrast, the C_6H_6/C_6F_6 mixture combines the capability of suspending graphene with the ability to remove the solvent by freeze-drying due to the high vapor pressure and high freezing point of the mixture.

Drop casting a liquid C_6H_6/C_6F_6 graphene suspension results in the immediate freezing of the suspension due to evaporative cooling. Solvent sublimation occurs with no additional cooling or vacuum required. Figure 5 is a field emission scanning electron microscope (FESEM) image of such a material. This graphene "sponge" contains no surfactants, polymer, or solvent residue and is continuous over the entire surface onto which it is cast.

Not surprisingly, the graphene sponge is weak mechanically, as it consists of a combination of multisheet stacks and single

dx.doi.org/10.1021/ja211225p | J. Am. Chem. Soc. 2012, 134, 5018−5021

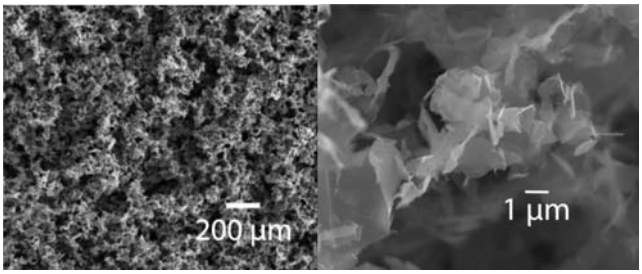

Figure 5. FESEM images of a three-dimensional graphene structure formed by freeze-drying a suspension of graphene from a hexafluorobenzene/benzene solvent mixture.

sheets held together by van der Waals forces. While the sponge morphology is related to the structure of the graphene suspension, the presence of multisheets stacks is not an indication that single sheets do not exist in the suspension. Separated graphene sheets, upon solvent removal, will restack. This is what occurs during freeze-drying, resulting in the jagged three-dimensional sponge structure held together by misaligned and interconnecting restacked graphene sheets, shown in Figure 5.

In this communication, we have presented a method for the dispersion of pristine graphene, both from natural flake graphene and HOPG. This method does not require the use of oxidized materials or materials that have been reduced after oxidation, meaning that nearly defect-free graphene can be recovered. It also does not require the use of strong (e.g., chlorosulfonic) acids.[38] Unlike the more common solvents such as DMF or NMP, the mixed solvent presented here is low boiling and thus easily removed. As an example of its utility, we describe the production of a high surface area, three-dimensional graphene sponge with potential applications for catalysis and electronics.[35−37,39−41]

■ ASSOCIATED CONTENT

Ⓢ Supporting Information

Experimental procedures, details of TEM and AFM sample preparation, and details of the computational study. This material is available free of charge via the Internet at http://pubs.acs.org.

■ AUTHOR INFORMATION

Corresponding Author

adamson@uconn.edu

Notes

The authors declare no competing financial interest.

■ ACKNOWLEDGMENTS

This work was supported by the Air Force Office of Scientific Research award number FA9550-10-0462 and by NSF DMR-1004576 and DMR-1111030. Resources of the Keeneland Computing Facility at the Georgia Institute of Technology, which is supported by the National Science Foundation under Contract OCI-0910735, were used in this research.

■ REFERENCES

(1) Singh, V.; Joung, D.; Zhai, L.; Das, S.; Khondaker, S. I.; Seal, S. *Prog. Mater. Sci.* **2011**, *56*, 1178.
(2) Allen, M. J.; Tung, V. C.; Kaner, R. B. *Chem. Rev.* **2010**, *110*, 132.
(3) Subrina, S.; Kotchetkov, D. *J. Nanoelectron. Optoelectron.* **2008**, *3*, 249.
(4) Geim, A. K. *Science* **2009**, *324*, 1530.
(5) Balandin, A. A.; Ghosh, S.; Bao, W.; Calizo, I.; Teweldebrhan, D.; Miao, F.; Lau, C. N. *Nano Lett.* **2008**, *8*, 902.
(6) Lee, C.; Wei, X.; Kysar, J. W.; Hone, J. *Science* **2008**, *321*, 385.
(7) Soldano, C.; Mahmood, A.; Dujardin, E. *Carbon* **2010**, *48*, 2127.
(8) Shih, C.-J.; Vijayaraghavan, A.; Krishnan, R.; Sharma, R.; Han, J.-H.; Ham, M.-H.; Jin, Z.; Lin, S.; Paulus, G. L. C.; Reuel, N. F.; Wang, Q. H.; Blankschtein, D.; Strano, M. S. *Nat. Nanotechnol.* **2011**, *6*, 439.
(9) Coleman, J. N. *Adv. Funct. Mater.* **2009**, *19*, 3680.
(10) Wang, J.; Manga, K. K.; Bao, Q.; Loh, K. P. *J. Am. Chem. Soc.* **2011**, *133*, 8888.
(11) Hamilton, C. E.; Lomeda, J. R.; Sun, Z.; Tour, J. M.; Barron, A. R. *Nano Lett.* **2009**, *9*, 3460.
(12) Williams, J. H.; Cockcroft, J. K.; Fitch, A. N. *Angew. Chem., Int. Ed.* **1992**, *31*, 1655.
(13) Schroer, J.; Monson, P. *J. Chem. Phys.* **2003**, *118*, 2815.
(14) Patrick, C.; Prosser, G. *Nature* **1960**, *187*, 1021.
(15) Bourlinos, A. B.; Georgakilas, V.; Zboril, R.; Steriotis, T. A.; Stubos, A. K. *Small* **2009**, *5*, 1841.
(16) Williams, J. H. *Acc. Chem. Res.* **1993**, *26*, 593.
(17) Tsuzuki, S.; Uchimaru, T.; Mikami, M. *J. Phys. Chem. A* **2006**, *110*, 2027.
(18) West, A. Jr; Mecozzi, S.; Dougherty, D. *J. Phys. Org. Chem.* **1997**, *10*, 347.
(19) Fowler, P.; Steiner, E. *J. Phys. Chem. A* **1997**, *101*, 1409.
(20) Coates, G.; Dunn, A.; Henling, L.; Ziller, J.; Lobkovsky, E.; Grubbs, R. *J. Am. Chem. Soc.* **1998**, *120*, 3641.
(21) Coates, G. W.; Dunn, A. R.; Henling, L. M.; Dougherty, D. A.; Grubbs, R. H. *Angew. Chem., Int. Ed.* **1997**, *36*, 248.
(22) Pugh, C.; Tang, C. N.; Paz-Pazos, M.; Samtani, O.; Dao, A. H. *Macromolecules* **2007**, *40*, 8178.
(23) Wolfs, M.; Darmanin, T.; Guittard, F. *Macromolecules* **2011**, *44*, 9286.
(24) Percec, V.; Glodde, M.; Peterca, M.; Rapp, A.; Schnell, I.; Spiess, H. W.; Bera, T. K.; Miura, Y.; Balagurusamy, V. S. K.; Aqad, E.; Heiney, P. A. *Chem.—Eur. J.* **2006**, *12*, 6298.
(25) Weck, M.; Dunn, A.; Matsumoto, K.; Coates, G.; Lobkovsky, E.; Grubbs, R. *Angew. Chem., Int. Ed.* **1999**, *38*, 2741.
(26) Kumar, S.; Rosenberg, J. M.; Bouzida, D.; Swendsen, R. H.; Kollman, P. A. *J. Comput. Chem.* **1995**, *16*, 1339.
(27) Good, R. J. *J. Adhes. Sci. Technol.* **1992**, *6*, 1269.
(28) Rafiee, J.; Rafiee, M. A.; Yu, Z.-Z.; Koratkar, N. *Adv. Mater.* **2010**, *22*, 2151.
(29) Bendure, R. *J. Colloid Interface Sci.* **1973**, *42*, 137.
(30) Jin, W.; Koplik, J.; Banavar. *Phys. Rev. Lett.* **1997**, *78*, 1520.
(31) Yaminsky, V.; Nylander, T.; Ninham, B. *Langmuir* **1997**, *13*, 1746.
(32) Marmur, A. *Ann. Rev. Mater. Res.* **2009**, *39*, 473.
(33) Di Mundo, R.; Palumbo, F. *Plasma Processes Polym.* **2010**, *8*, 14.
(34) Fadeev, A. Y.; McCarthy, T. J. *Langmuir* **1999**, *15*, 7238.
(35) Liu, F.; Seo, T. S. *Adv. Funct. Mater.* **2010**, *20*, 1930.
(36) Vickery, J. L.; Patil, A. J.; Mann, S. *Adv. Mater.* **2009**, *21*, 2180.
(37) Yuan, Q.; Hu, H.; Gao, J.; Ding, F.; Liu, Z.; Yakobson, B. I. *J. Am. Chem. Soc.* **2011**, *133*, 16072.
(38) Behabtu, N.; Lomeda, J. R.; Green, M. J.; Higginbotham, A. L.; Sinitskii, A.; Kosynkin, D. V.; Tsentalovich, D.; Parra-Vasquez, A. N. G.; Schmidt, J.; Kesselman, E.; Cohen, Y.; Talmon, Y.; Tour, J. M.; Pasquali, M. *Nat. Nanotechnol.* **2010**, *5*, 406.
(39) Gutiérrez, M. C.; Ferrer, M. L.; del Monte, F. *Chem. Mater.* **2008**, *20*, 634.
(40) Gutierrez, M. C.; Hortiguela, M. J.; Amarilla, J. M.; Jimenez, R.; Ferrer, M. L.; delMonte, F. *J. Phys. Chem. C* **2007**, *111*, 5557.
(41) Xu, Z.; Gao, C. *ACS Nano* **2011**, *5*, 2908.